

# New analysis of the SN 1987A neutrinos with a flexible spectral shape

Alessandro Mirizzi<sup>1,2</sup> and Georg G. Raffelt<sup>1</sup>

<sup>1</sup>Max-Planck-Institut für Physik (Werner-Heisenberg-Institut), Föhringer Ring 6, 80805 München, Germany

<sup>2</sup>Dipartimento di Fisica and Sezione INFN di Bari, Via Amendola 173, 70126 Bari, Italy

(Dated: July 17, 2018)

We analyze the neutrino events from the supernova (SN) 1987A detected by the Kamiokande II (KII) and Irvine-Michigan-Brookhaven (IMB) experiments. For the time-integrated flux we assume a quasi-thermal spectrum of the form  $(E/E_0)^\alpha e^{-(\alpha+1)E/E_0}$  where  $\alpha$  plays the role of a spectral index. This simple representation not only allows one to fit the total energy  $E_{\text{tot}}$  emitted in  $\bar{\nu}_e$  and the average energy  $\langle E_{\bar{\nu}_e} \rangle$ , but also accommodates a wide range of shapes, notably anti-pinch spectra that are broader than a thermal distribution. We find that the pile-up of low-energy events near threshold in KII forces the best-fit value for  $\alpha$  to the lowest value of any assumed prior range. This applies to the KII events alone as well as to a common analysis of the two data sets. The preference of the data for an “unphysical” spectral shape implies that one can extract meaningful values for  $\langle E_{\bar{\nu}_e} \rangle$  and  $E_{\text{tot}}$  only if one fixes a prior value for  $\alpha$ . The tension between the KII and IMB data sets and theoretical expectations for  $\langle E_{\bar{\nu}_e} \rangle$  is not resolved by an anti-pinch spectrum.

PACS numbers: 14.60.Pq, 95.55.Vj, 95.85.Ry, 97.60.Bw

## I. INTRODUCTION

The neutrino observations of supernova (SN) 1987A [1–6] have long been taken as a confirmation of the salient features of our physical understanding of the core-collapse SN phenomenon. At the same time, a detailed interpretation [7–14] of the data is difficult because of a number of “anomalies” [15]. In particular, the energy spectra implied by the Kamiokande II (KII) and Irvine-Michigan-Brookhaven (IMB) events are barely consistent with each other. Moreover, the average  $\bar{\nu}_e$  energy implied by KII is much lower than expected from numerical simulations. The energies implied by IMB alone would be compatible with theoretical models, but the results of a common KII and IMB analysis are difficult to square with expectations.

In the presence of neutrino oscillations, the  $\bar{\nu}_e$  flux observed in a detector is a superposition of the  $\bar{\nu}_e$  and  $\bar{\nu}_{\mu,\tau}$  fluxes produced at the source. Therefore, the KII and IMB detectors may have observed different fluxes because the SN 1987A neutrinos have traversed different sections of the Earth so that matter effects can modify the observed superposition of source spectra [16, 17]. However, it is expected that  $\langle E_{\bar{\nu}_{\mu,\tau}} \rangle > \langle E_{\bar{\nu}_e} \rangle$  so that oscillations aggravate the tension between observed and expected  $\bar{\nu}_e$  energies [11, 16, 17]. In any event, the differences between  $\langle E_{\bar{\nu}_{\mu,\tau}} \rangle$  and  $\langle E_{\bar{\nu}_e} \rangle$  are probably much smaller than had been thought previously [28–30] so that the Earth matter effect is no longer expected to cause gross modifications of the observed  $\bar{\nu}_e$  spectrum. Of course, the relatively subtle modifications caused by Earth matter effects can be crucial for identifying the neutrino mass ordering from the high-statistics neutrino signal of a future galactic SN [18–27].

Previous studies of the SN 1987A neutrinos usually assumed a thermal spectrum and then extracted  $\langle E_{\bar{\nu}_e} \rangle$  and the overall flux from the individual detector signals or from a combined analysis. One exception is the analysis

of Janka and Hillebrandt [9] who assumed an effective Fermi-Dirac distribution of the form

$$\varphi(E) \propto \frac{E^2}{e^{E/T-\eta} + 1}, \quad (1)$$

where  $T$  is an effective temperature and  $\eta$  a degeneracy parameter. In their maximum-likelihood analysis they allowed only for positive values of  $\eta$ . With this prior they found a best-fit value of  $\eta = 0$  for both the KII and IMB data sets, suggesting that the data prefer the broadest allowed distribution compatible with the prior range for  $\eta$ . However, even allowing for negative values for  $\eta$  would not have changed these results because  $\eta \rightarrow -\infty$  corresponds to a Maxwell-Boltzmann spectrum, differing only marginally from the Fermi-Dirac case with  $\eta = 0$ .

The main purpose of our new study is to investigate if better internal agreement of the SN 1987A data as well as better agreement between the data and theoretical expectations can be achieved if a more flexible representation of the spectral shape is assumed. Numerical studies of neutrino transport suggest that the instantaneous spectra are “pinched,” i.e. that they are narrower than a thermal spectrum [9, 29]. A pinched spectrum can be represented by a Fermi-Dirac distribution with positive  $\eta$ . However, the SN 1987A data measure the time-integrated spectrum, i.e. a superposition of instantaneous spectra with varying average energies. Therefore, the integrated spectrum may well be broader, not narrower, than a thermal spectrum, i.e. it may well be anti-pinch.

If the time-integrated spectrum is quasi-thermal in the sense that it rises from zero for low energies, reaches a maximum, and has a long tail to high energies, then the simplest conceivable representation is [29]

$$\varphi(E) = \frac{1}{E_0} \frac{(\alpha+1)^{(\alpha+1)}}{\Gamma(\alpha+1)} \left(\frac{E}{E_0}\right)^\alpha \exp\left[-(\alpha+1)\frac{E}{E_0}\right], \quad (2)$$

where  $\int \varphi(E) dE = 1$  and  $E_0$  is an energy scale with the property  $\langle E \rangle = E_0$ . The numerical parameter  $\alpha$  controls

the width of the distribution,

$$\frac{\langle E^2 \rangle - \langle E \rangle^2}{\langle E \rangle^2} = \frac{1}{1 + \alpha}. \quad (3)$$

We note that  $\alpha = 2$  corresponds to a Maxwell-Boltzmann spectrum,  $\alpha > 2$  to a pinched spectrum with suppressed high- and low-energy tails, and  $\alpha < 2$  to an anti-pinched spectrum. For  $\alpha \rightarrow \infty$  the spectrum becomes  $\delta(E - E_0)$ . Since the oscillations effect on the detected  $\bar{\nu}_e$  spectrum is reasonably small (see Sec. I), it makes sense to fit directly the effective  $\bar{\nu}_e$  spectrum, *after* the oscillations, with the distribution of Eq. (2).

In Sec. II we present the SN 1987A neutrino data and perform a new maximum-likelihood analysis. A summary and conclusions are given in Sec. III.

## II. MAXIMUM-LIKELIHOOD ANALYSIS

### A. SN 1987A Data

We limit our analysis to the SN 1987A data of the KII [1, 2] and IMB [3, 4] detectors that measure SN neutrinos almost exclusively by the inverse beta reaction  $\bar{\nu}_e + p \rightarrow n + e^+$ . We show the measured positron spectra in Fig. 1 where we have left out the KII event No. 6 that is attributed to background. In Table I we summarize the properties of the neutrino signal in the two detectors. We do not include the Baksan Scintillator Telescope (BST) data [5, 6] because it is much more uncertain which of

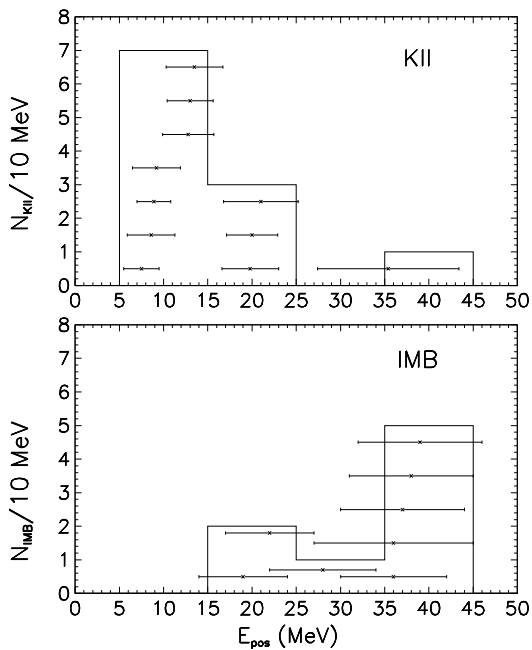


FIG. 1: Positron spectra detected at KII (upper panel) and IMB (lower panel) in connection with SN 1987A. We also show the energies of the individual events together with their experimental errors.

TABLE I: Number of SN 1987A events and average positron energies at the KII and IMB detectors.

| Detector | $N_{\text{events}}$ | $\langle E_{e^+} \rangle$ [MeV] |
|----------|---------------------|---------------------------------|
| KII      | 11                  | $15.4 \pm 1.1$                  |
| IMB      | 8                   | $31.9 \pm 2.3$                  |

the events have to be attributed to background, i.e. in a maximum-likelihood analysis one would have to model the background. This requires to use the time structure of the neutrino burst [13, 14], whereas we limit our study to the time-integrated flux.

### B. Maxwell-Boltzmann Spectrum

We perform a maximum-likelihood analysis of the SN 1987A signal along the lines of the previous literature such as Ref. [11]. For the detection cross section we use an updated analytic fit [31] and for the detection efficiencies we use the analytic fit functions of Ref. [32].

In order to compare with the previous literature we first consider a Maxwell-Boltzmann  $\bar{\nu}_e$  spectrum, i.e. we use  $\alpha = 2$  in Eq. (2). As fit parameters we use the average  $\bar{\nu}_e$  energy  $E_0$  and the total energy  $E_{\text{tot}}$  emitted by SN 1987A in the form of  $\bar{\nu}_e$ . Of course, these parameters refer to the spectrum measured in the detectors after the partial flavor swapping caused by neutrino oscillations. Our results shown in Fig. 2 agree with the previous literature and illustrate once more the tension between the average energies implied by the two detectors.

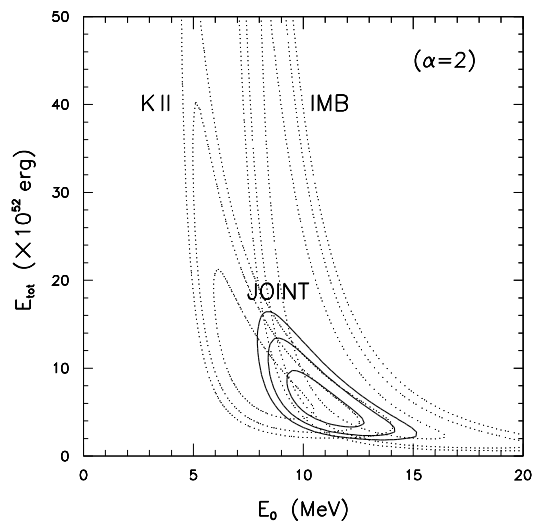


FIG. 2: Contours of constant likelihood that correspond to 68.3%, 95% and 99% C.L. in the plane  $E_0 - E_{\text{tot}}$  for an assumed Maxwell-Boltzmann  $\bar{\nu}_e$  spectrum, corresponding to  $\alpha = 2$  in Eq. (2). The dotted lines refer to the KII and IMB signals, respectively, whereas the solid lines represent a joint analysis.

### C. General Spectrum

Next we use a general spectrum of the form Eq. (2) with  $E_0$ ,  $E_{\text{tot}}$ , and  $\alpha$  as our fit parameters with a prior  $\alpha \geq 0$ . We show the best-fit values for these parameters as well as the implied event numbers and average positron energies in the detectors in Table II. This analysis is performed for each detector separately as well as for the joint case.

TABLE II: Best-fit values for  $E_{\text{tot}}$  in  $10^{52}$  erg,  $E_0$  in MeV, and  $\alpha$  based on the indicated data sets. The implied characteristics of the expected detector signals are also shown.

| Data Set | Best-fit param's |       |          | KII                 |                           | IMB                 |                           |
|----------|------------------|-------|----------|---------------------|---------------------------|---------------------|---------------------------|
|          | $E_{\text{tot}}$ | $E_0$ | $\alpha$ | $N_{\text{events}}$ | $\langle E_{e^+} \rangle$ | $N_{\text{events}}$ | $\langle E_{e^+} \rangle$ |
| KII      | 17.4             | 3.7   | 0.0      | 10.9                | 15.3                      | 1.3                 | 27.5                      |
| IMB      | 1.1              | 30.6  | 60.0     | 6.6                 | 30.3                      | 7.9                 | 31.4                      |
| Joint    | 10.1             | 5.4   | 0.0      | 14.1                | 19.2                      | 4.9                 | 32.0                      |

The IMB data alone prefer a functional form with a very large value for  $\alpha$ , i.e. essentially a  $\delta$  function. This behavior is intuitively obvious because 5 of the 8 IMB events have positron energies in the very narrow range 36–39 MeV. The KII data alone, on the other hand, prefer  $\alpha = 0$ , i.e. a huge total flux of low-energy  $\bar{\nu}_e$ . The pile-up of events just above the KII threshold of 7.5 MeV implies that the turn-over at low energies of a quasi-thermal spectrum is not visible in the data, which are sensitive only to the decreasing higher energy tail of the spectrum. This feature is reproduced in the likelihood by pushing  $E_0$  toward low values and broadening as much as possible the width. Moreover, the low value of  $E_0$  is compensated by a huge amount of the total emitted energy  $E_{\text{tot}}$ . We have checked that even when we allow for negative  $\alpha$  values the maximum of the likelihood always coincides with the lowest allowed value. Of course, for  $\alpha \leq -1$  the total neutrino flux diverges.

Contrary to our expectation, this behavior remains the same for a joint analysis of the two data sets, even though the total flux is smaller and the average  $\bar{\nu}_e$  energy is larger.

In Fig. 3 we show the difference  $\Delta \ln \mathcal{L}$  relative to the best-fit value as a function of  $\alpha$  for the two separate data sets and the joint analysis. In all cases we have marginalized over the parameters  $E_0$  and  $E_{\text{tot}}$ . The 95% C.L. allowed range for a single degree of freedom corresponds to  $\Delta \ln \mathcal{L} = 1.92$  shown as a horizontal dot-dashed line in Fig. 3. Evidently IMB alone has no strong preference for any spectral shape. The 95% upper limit on  $\alpha$  is lower for the combined data than for KII alone because the combined data also prefer a larger  $E_0$  and lower total flux. Overall, the data do not distinguish in a useful way between different plausible spectral shapes. In particular, the data do not prefer a quasi-thermal spectrum but rather a monotonically falling one, in contrast with plausible expectations.

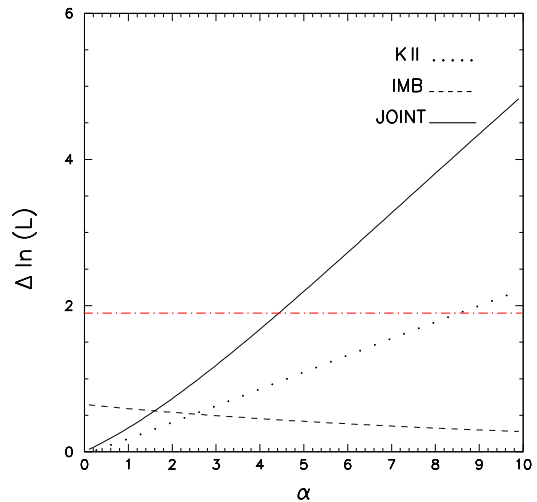


FIG. 3: Curves of  $\Delta \ln \mathcal{L}$  relative to the best-fit value as a function of  $\alpha$  for KII (dotted line), IMB (dashed line) and for the joint data set (continuous line). The 95% C.L. for  $\alpha$  is indicated with the dot-dashed horizontal line. We have marginalized over  $E_0$  and  $E_{\text{tot}}$ .

### D. Fixed Prior Values for $\alpha$

We conclude that in order to extract information on the average  $\bar{\nu}_e$  energy and the total flux it is not useful to marginalize over the parameter  $\alpha$  because the result depends sensitively on the assumed prior range for  $\alpha$  and because unphysically low values are preferred by the data. Therefore, we return to fixing the spectral shape in advance and analyze the data for different choices of  $\alpha$ . In Fig. 4 we show the 95% C.L. contours in the  $E_0$ - $E_{\text{tot}}$  plane for  $\alpha = 0, 2$  and  $4$  where the case  $\alpha = 2$  is identical with the 95% C.L. shown in Fig. 2. Larger values of  $\alpha$  (pinched spectra) increase the range of average energies and bring them closer to theoretical expectations, but at the same time decrease the range of overlap between IMB

TABLE III: Best-fit values for  $E_{\text{tot}}$  in  $10^{52}$  erg and  $E_0$  in MeV for the indicated fixed choices of  $\alpha$ . The implied characteristics of the expected detector signals are also shown.

| $\alpha$     | Data Set | Best-fit         |       | KII                 |                           | IMB                 |                           |
|--------------|----------|------------------|-------|---------------------|---------------------------|---------------------|---------------------------|
|              |          | $E_{\text{tot}}$ | $E_0$ | $N_{\text{events}}$ | $\langle E_{e^+} \rangle$ | $N_{\text{events}}$ | $\langle E_{e^+} \rangle$ |
| $\alpha = 0$ | KII      | 17.4             | 3.7   | 10.9                | 15.3                      | 1.3                 | 27.5                      |
|              | IMB      | 23.7             | 5.0   | 28.7                | 18.3                      | 8.0                 | 30.8                      |
|              | Joint    | 10.1             | 5.4   | 14.1                | 19.2                      | 4.9                 | 32.0                      |
| $\alpha = 2$ | KII      | 8.9              | 7.9   | 11.0                | 15.3                      | 1.1                 | 26.7                      |
|              | IMB      | 8.2              | 11.6  | 20.6                | 20.1                      | 8.0                 | 30.9                      |
|              | Joint    | 5.9              | 11.2  | 14.0                | 19.5                      | 4.9                 | 30.3                      |
| $\alpha = 4$ | KII      | 6.6              | 10.2  | 11.0                | 15.4                      | 1.0                 | 25.3                      |
|              | IMB      | 4.7              | 15.9  | 16.3                | 21.8                      | 8.0                 | 31.0                      |
|              | Joint    | 4.7              | 14.2  | 14.1                | 19.8                      | 4.8                 | 29.5                      |

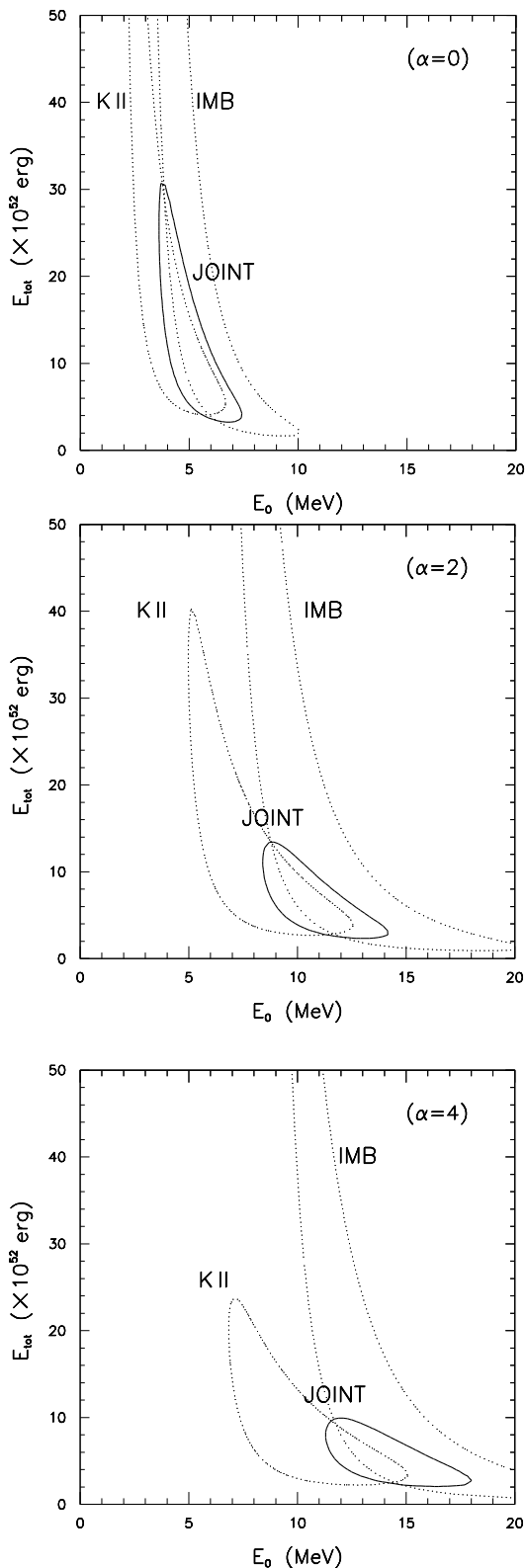


FIG. 4: Contours of 95 % C.L. in the plane of  $E_0$  and  $E_{tot}$  for  $\alpha = 0$  (top panel),  $\alpha = 2$  (middle) and  $\alpha = 4$  (bottom). The dotted lines are for KII and IMB separately whereas the solid line is for the joint data set.

and KII. In Table III we show the best-fit parameters  $E_0$  and  $E_{tot}$  for the three  $\alpha$  cases and different data sets as well as the implied signal characteristics.

### III. DISCUSSION AND SUMMARY

The expected neutrino energies from core-collapse SNe are of practical importance for sensitivity forecasts of a future galactic SN neutrino detection, in particular with regard to neutrino mixing parameters [18–27]. The expected energies are also important in the context of current limits and future detection possibilities of the diffuse SN neutrino background from all SNe in the universe [33–37]. The internal tension within the SN 1987A neutrino data as well as the tension with theoretical expectations has persuaded most workers in this field to ignore the data and rely on the output of numerical simulations even though current SN theory may still be missing an important piece of input physics to obtain robust explosions [38].

One explanation for the tension between the KII and IMB data is that the detectors actually observed different spectra due to the Earth matter effect [16, 17]. However, our current understanding of flavor-dependent neutrino spectra formation suggests that the flavor-dependent average energies in the anti-neutrino sector are not very different [28, 29]. Moreover, if the observed  $\bar{\nu}_e$  had been born as higher-energy  $\bar{\nu}_{\mu,\tau}$  at the source, the tension between theoretically expected and actually observed  $\bar{\nu}_e$  energies would be worse.

Loredo and Lamb [14] have tested a large variety of neutrino emission models and in particular have included what amounts to a bi-modal spectral shape that contains a lower-energy component attributed to the SN accretion phase and a higher-energy one attributed to the neutron-star cooling phase. They stress that such a spectral form is strongly favored by the data relative to a single-mode thermal spectrum. However, numerical simulations do not predict a bimodal spectrum because the average energies continuously increase from the accretion to the neutron-star cooling phase and at late times decrease again. Therefore, the spectral shape of the time-integrated flux does not seem to exhibit a bi-modal form but rather is expected to be a broadened quasi-thermal spectrum.

Motivated by this observation we have analysed the SN 1987A data, assuming a quasi-thermal spectrum of the general form Eq. (2) that is flexible enough to accommodate a continuum of spectral shapes from narrow (pinched) to broadened (anti-pinched) spectra relative to a Maxwell-Boltzmann distribution.

Perhaps unsurprisingly in view of the tension between the KII and IMB data, we find that the broadest possible distribution allowed by the chosen prior range of  $\alpha$  is preferred. In this way the tension between the data sets is somewhat reduced, but at the same time the average  $\bar{\nu}_e$  energies are pulled to lower values, thus exacerbat-

ing the tension with the output of representative numerical simulations. (The average neutrino energies found in many different numerical simulations have been collected in Ref. [29].)

Assuming the time-integrated neutrino flux from a SN indeed exhibits a quasi-thermal spectrum roughly of the form Eq. (2), the implied average  $\bar{\nu}_e$  energies and total emitted energy depend sensitively on the chosen prior range for  $\alpha$ . The data themselves prefer the smallest possible  $\alpha$ -values, i.e. not a quasi-thermal spectrum but rather a monotonically falling one. The assumption of a realistic quasi-thermal spectrum is not simultaneously consistent with typical theoretical expectations for  $\langle E_{\bar{\nu}_e} \rangle$  as well as the separate data sets from IMB and KII. Therefore, it remains unresolved if the SN 1987A data or theoretical simulations give us better benchmarks for the average  $\bar{\nu}_e$  energies to be used, for example, in the context of searches for the cosmic diffuse SN neutrino background.

It appears that the question of the true neutrino spectrum from a typical SN can be empirically resolved only by the high-statistics signal from a future galactic SN or by the patient accumulation of data on a neutrino-by-neutrino basis from SNe in nearby galaxies [39].

### Acknowledgments

We acknowledge partial support by the Deutsche Forschungsgemeinschaft under Grant No. SFB-375 and by the European Union under the Ilias project, contract No. RII3-CT-2004-506222. The work of A.M. is supported in part by the Italian “Istituto Nazionale di Fisica Nucleare” (INFN) and by the “Ministero dell’Istruzione, Università e Ricerca” (MIUR) through the “Astroparticle Physics” research project.

- 
- [1] K. Hirata *et al.* (Kamiokande-II Collaboration), “Observation of a neutrino burst from the supernova SN 1987A,” *Phys. Rev. Lett.* **58**, 1490 (1987).
- [2] K. S. Hirata *et al.*, “Observation in the Kamiokande-II detector of the neutrino burst from supernova SN 1987A,” *Phys. Rev. D* **38**, 448 (1988).
- [3] R. M. Bionta *et al.*, “Observation of a neutrino burst in coincidence with supernova SN 1987A in the Large Magellanic Cloud,” *Phys. Rev. Lett.* **58**, 1494 (1987).
- [4] C. B. Bratton *et al.* [IMB Collaboration], “Angular distribution of events from SN 1987A,” *Phys. Rev. D* **37**, 3361 (1988).
- [5] E. N. Alekseev, L. N. Alekseeva, V. I. Volchenko and I. V. Krivosheina, “Possible detection of a neutrino signal on 23 February 1987 at the Baksan underground scintillation telescope of the Institute of Nuclear Research,” *JETP Lett.* **45**, 589 (1987) [*Pisma Zh. Eksp. Teor. Fiz.* **45**, 461 (1987)].
- [6] E. N. Alekseev, L. N. Alekseeva, I. V. Krivosheina and V. I. Volchenko, “Detection of the neutrino signal from SN 1987A in the LMC using the INR Baksan underground scintillation telescope,” *Phys. Lett. B* **205**, 209 (1988).
- [7] J. N. Bahcall, T. Piran, W. H. Press and D. N. Spergel, “Neutrino temperatures and fluxes from the LMC supernova,” *Nature* **327**, 682 (1987).
- [8] L. M. Krauss, “Neutrino spectroscopy of the supernova SN 1987A,” *Nature* **329**, 689 (1987).
- [9] H. T. Janka and W. Hillebrandt, “Neutrino emission from type II supernovae: An analysis of the spectra,” *Astron. Astrophys.* **224**, 49 (1989).
- [10] P. J. Kernan and L. M. Krauss, “Updated limits on the electron neutrino mass and large angle oscillations from SN 1987A,” *Nucl. Phys. B* **437**, 243 (1995) [*astro-ph/9410010*].
- [11] B. Jegerlehner, F. Neubig and G. Raffelt, “Neutrino Oscillations and the Supernova 1987A Signal,” *Phys. Rev. D* **54**, 1194 (1996) [*astro-ph/9601111*].
- [12] M. Kachelriess, R. Tomàs and J. W. F. Valle, “Large lepton mixing and supernova 1987A,” *JHEP* **0101**, 030 (2001) [*hep-ph/0012134*].
- [13] T. J. Loredo and D. Q. Lamb, “Neutrinos from SN 1987A: Implications for cooling of the nascent neutron star and the mass of the electron anti-neutrino,” *Ann. N.Y. Acad. Sci.* **571**, 601 (1989).
- [14] T. J. Loredo and D. Q. Lamb, “Bayesian analysis of neutrinos observed from supernova SN 1987A,” *Phys. Rev. D* **65**, 063002 (2002) [*astro-ph/0107260*].
- [15] G. G. Raffelt, *Stars as laboratories for fundamental physics* (University of Chicago Press, 1996).
- [16] C. Lunardini and A. Y. Smirnov, “Neutrinos from SN 1987A, Earth matter effects and the LMA solution of the solar neutrino problem,” *Phys. Rev. D* **63**, 073009 (2001) [*hep-ph/0009356*].
- [17] C. Lunardini and A. Y. Smirnov, “Neutrinos from SN 1987A: Flavor conversion and interpretation of results,” *Astropart. Phys.* **21**, 703 (2004) [*hep-ph/0402128*].
- [18] A. S. Dighe and A. Y. Smirnov, “Identifying the neutrino mass spectrum from the neutrino burst from a supernova,” *Phys. Rev. D* **62**, 033007 (2000) [*hep-ph/9907423*].
- [19] K. Takahashi, M. Watanabe, K. Sato and T. Totani, “Effects of neutrino oscillation on the supernova neutrino spectrum,” *Phys. Rev. D* **64**, 093004 (2001) [*hep-ph/0105204*].
- [20] K. Takahashi and K. Sato, “Earth effects on supernova neutrinos and their implications for neutrino parameters,” *Phys. Rev. D* **66**, 033006 (2002) [*hep-ph/0110105*].
- [21] H. Minakata, H. Nunokawa, R. Tomàs and J. W. F. Valle, “Probing supernova physics with neutrino oscillations,” *Phys. Lett. B* **542**, 239 (2002) [*hep-ph/0112160*].
- [22] A. S. Dighe, M. T. Keil and G. G. Raffelt, “Detecting the neutrino mass hierarchy with a supernova at IceCube,” *JCAP* **0306**, 005 (2003) [*hep-ph/0303210*].
- [23] A. S. Dighe, M. T. Keil and G. G. Raffelt, “Identifying Earth matter effects on supernova neutrinos at a single detector,” *JCAP* **0306**, 006 (2003) [*hep-ph/0304150*].
- [24] A. S. Dighe, M. Kachelriess, G. G. Raffelt and R. Tomàs, “Signatures of supernova neutrino oscillations in the

- Earth mantle and core,” JCAP **0401**, 004 (2004) [hep-ph/0311172].
- [25] C. Lunardini and A. Y. Smirnov, “Probing the neutrino mass hierarchy and the 13-mixing with supernovae,” JCAP **0306**, 009 (2003) [hep-ph/0302033].
- [26] G. L. Fogli, E. Lisi, A. Mirizzi and D. Montanino, “Probing supernova shock waves and neutrino flavor transitions in next-generation water-Cherenkov detectors,” JCAP **0504**, 002 (2005) [hep-ph/0412046].
- [27] R. Tomàs, M. Kachelriess, G. Raffelt, A. Dighe, H.-T. Janka and L. Scheck, “Neutrino signatures of supernova shock and reverse shock propagation,” JCAP **0409**, 015 (2004) [astro-ph/0407132].
- [28] G. G. Raffelt, “Mu- and tau-neutrino spectra formation in supernovae,” Astrophys. J. **561**, 890 (2001) [astro-ph/0105250].
- [29] M. T. Keil, G. G. Raffelt and H.-T. Janka, “Monte Carlo study of supernova neutrino spectra formation,” Astrophys. J. **590**, 971 (2003) [astro-ph/0208035].
- [30] G. G. Raffelt, M. T. Keil, R. Buras, H.-T. Janka and M. Rampp, “Supernova neutrinos: Flavor-dependent fluxes and spectra,” Proc. of the 4th Workshop on Neutrino Oscillations and their Origin: NooN 2003 (10–14 February 2003, Kanazawa, Japan), edited by Y. Suzuki, M. Nakahata, Y. Itow, M. Shiozawa and Y. Obayashi (World Scientific, Singapore, 2004), pp. 380–387 [astro-ph/0303226].
- [31] A. Strumia and F. Vissani, “Precise quasielastic neutrino nucleon cross section,” Phys. Lett. B **564**, 42 (2003) [astro-ph/0302055].
- [32] A. Burrows, “Supernova Neutrinos,” Astrophys. J. **334**, 891 (1988).
- [33] M. Malek *et al.* (Super-Kamiokande Collab.), “Search for supernova relic neutrinos at Super-Kamiokande,” Phys. Rev. Lett. **90**, 061101 (2003) [hep-ex/0209028].
- [34] S. Ando and K. Sato, “Relic neutrino background from cosmological supernovae,” New J. Phys. **6**, 170 (2004) [astro-ph/0410061].
- [35] L. E. Strigari, J. F. Beacom, T. P. Walker and P. Zhang, “The concordance cosmic star formation rate: Implications from and for the supernova neutrino and gamma ray backgrounds,” JCAP **0504**, 017 (2005) [astro-ph/0502150].
- [36] G. L. Fogli, E. Lisi, A. Mirizzi and D. Montanino, “Three-generation flavor transitions and decays of supernova relic neutrinos,” Phys. Rev. D **70**, 013001 (2004) [hep-ph/0401227].
- [37] J. F. Beacom and L. E. Strigari, “New Test of Supernova Electron Neutrino Emission using Sudbury Neutrino Observatory Sensitivity to the Diffuse Supernova Neutrino Background,” [hep-ph/0508202].
- [38] R. Buras, M. Rampp, H.-T. Janka and K. Kifonidis, “Improved models of stellar core collapse and still no explosions: What is missing?,” Phys. Rev. Lett. **90**, 241101 (2003) [astro-ph/0303171].
- [39] S. Ando, J. F. Beacom and H. Yüksel, “Detection of neutrinos from supernovae in nearby galaxies,” [astro-ph/0503321].